

# Image Compressed Sensing Recovery Using Intra-Block Prediction

*Diana Mandache, Ali Akbari and Maria Trocan*

**Abstract** — Considering the strong correlation among the neighboring areas in an image, in this paper, we propose a compressed sensing recovery of images by providing an intra-block prediction for the image. Starting from an initial, direct compressed-sensed reconstruction and splitting it into non-overlapping blocks, a prediction for every block within the image is built up based on the average of its most similar neighboring blocks. An enhanced recovery of the image is obtained by adding the reconstructed residual -obtained as difference between the measurements of the original image and the obtained measurements of its prediction image- to the generated prediction. Experimental results show that the proposed algorithm outperforms, both subjectively and quantitatively, the direct reconstruction using the initial measurements alone.

**Keywords** — Block Prediction, Compressed Sensing, Image Reconstruction, Sparse Recovery.

## I. INTRODUCTION

COMPRESSED sensing (CS) is a signal acquisition method that can ensure full reconstruction using just a small amount of the random samples, unlike the traditional point-by-point sampling (Nyquist sampling theorem) [1]-[2]. Given the signal  $x \in \mathbb{R}^N$ , we obtain the measurements  $y \in \mathbb{R}^M$  by

$$y = \Phi x, \quad (1)$$

where  $\Phi$  is a  $M \times N$  random orthonormal matrix, called measurement basis. The subsampling rate is  $S = M/N$ , where  $M < N$ . Although the number of unknowns is larger than the number of measurements, the signal  $x$  can still be exactly recovered from  $y$ , if it is sparse enough [1]; this is the fundamental concept of CS theory. Sparsity can be achieved by applying a sparsity transform (such as discrete wavelet transform) to  $x$ ,

$$X = \Psi x, \quad (2)$$

where  $X$  represents the transform coefficients. The reconstruction of  $x$  from  $y$  is then accomplished in the transform domain. It should be noted that  $\Phi$  and  $\Psi$  have to be incoherent and  $M$  large enough [2].

How to efficiently reconstruct the image with the good recovery quality and the low computational complexity is always a focused topic in the CS applications fields. To

Authors are with the department of Signal, Images and Telecommunications (SITe), Institut Supérieur d'Électronique de Paris, 28 rue Notre Dame des Champs, Paris, France. (E-mail: {diana.mandache, ali.akbari, maria.trocan}@isep.fr).

address these issues, there have been some great efforts to develop the CS reconstruction algorithms which differ based on their computational complexity and reconstruction quality. The algorithm proposed in [3] is one of the outstanding CS reconstruction procedures which searches for the  $X$  with the smallest  $l_1$  norm consistent with the observed  $y$ ,

$$X = \arg \min_X \|X\|_1 \quad s.t. \quad y = \Phi \Psi^{-1} X. \quad (3)$$

Because of the high computational complexity of this procedure, the Smooth Projected Landweber (SPL) algorithm [4] has been proposed which provides a reduced computational complexity as well as having good reconstruction quality.

In the case of images and videos, saving the measurement matrix  $\Phi$  requires a large space of memory; moreover, it increases the computational burden during the reconstruction. Block compressed sensing (BCS) comes to solve these issues by splitting the image into  $B \times B$  distinct blocks and acquiring all the blocks using the same measurement matrix  $\Phi_B$ . Assuming  $x_i$  is the raster-scan representation of block  $i$  of the input image, the corresponding measurements is

$$y_i = \Phi_B x_i. \quad (4)$$

This procedure can be applied directly on the entire image by creating the block-diagonal matrix  $\Phi = \text{diag}(\Phi_B, \dots, \Phi_B)$  [4].

To make use of the block structure in order to achieve better recovery performance, several block-based approaches [4]-[8] have been proposed. The Block Compressed Sensing with Smoothed Projected Landweber (BCS-SPL) proposed in [4] recovers the signal using an iterative procedure, and adding Wiener filtering for removing blocking artifacts and a hard thresholding process for ensuring the signal sparsity.

In [9], it is demonstrated that the performance of the CS reconstruction is improved by access to the side information, for instance, having a similar signal to the target signal. In [10]-[12], we proposed the use of the disparity estimation and disparity compensation methods for generation a signal similar to each view in a multiview CS reconstruction system. Instead of fully reconstructing the current frame, only the residual between it and its prediction is reconstructed.

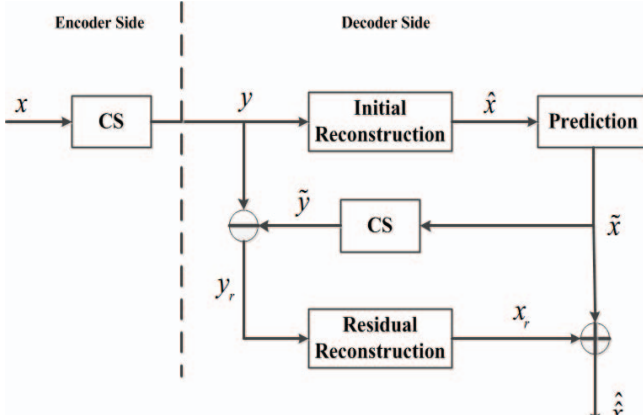


Fig.1. Block diagram of the proposed wavelet-domain residual based CS reconstruction

Different from our previous approach [12], in the proposed algorithm, we adopt the framework of the intra-image prediction and propose a novel strategy for the block-based CS reconstruction. We focus on exploiting the fundamental property of the CS theory which states that a very sparse signal can be perfectly reconstructed; in this sense we try to obtain a prediction comparable to the original image in order to have a residual so sparse that its recovery is able to enhance the quality of the image.

The proposed algorithm starts by an initial reconstruction of the image, using a direct (known) CS reconstruction method. By partitioning this initial image recovery into non-overlapping blocks of the same size, we use a local intra-block prediction of each block, based on the average of its most similar neighboring blocks, to calculate an accurate prediction of the image.

Experimental results show that the proposed method provides a significant increase in the reconstruction quality as compared to the direct CS reconstruction of the image [4].

The remainder of the paper is organized as follows. Section II introduces the basics for our method. Experimental results demonstrating the efficiency of the proposed scheme are presented in section III. Finally, some concluding remarks are made in section IV.

## II. PROPOSED METHOD

In the sequel, we investigate the adaption of the proposed residual-based CS reconstruction into the existing algorithms. A high quality recovery of the image is obtained using the proposed algorithm, denoted as Block Residual based CS recovery (BRCS) in the followings, by adapting an accurate prediction into the classical direct CS recovery methods.

The overall flowchart of the proposed system is depicted in Figure 1. At the encoder side, the image is sampled by (1) with a  $M \times N$  Gaussian measurement matrix  $\Phi$  at a certain substrate,  $S = M/N$ , producing the measurements  $y$ .

The core idea behind the proposed CS reconstructed technique is to exploit the high level of correlation among the neighboring blocks in an image. The image is

$b_1$	$b_2$	$b_3$
$b_4$	$b$	$b_5$
$b_6$	$b_7$	$b_8$

Fig. 2. Block  $b$  and its 8 neighbors

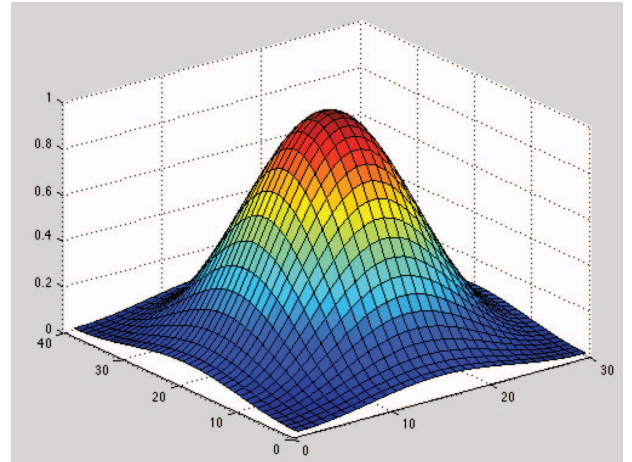


Fig. 3. Hamming weighting function

reconstructed from the measurements  $y$  by using a two phase process explained in the sequel. First step is the initial recovery of the image, whereas second one is the enhancement stage for improving the final quality of image.

### Phase 1: Initial phase

Initially, the image is reconstructed from the received measurements  $y$  to produce  $\hat{x}$ . The reconstruction of the image can be obtained by different algorithms. We select the BCS-SPL algorithm [4] for its high performance and low complexity in reconstruction of the initial image.

### Phase 2: Enhancement phase

In this phase, a measurement-domain residual is generated for the image using the received measurements  $y$  and a prediction  $\hat{x}$  of the image.

Moving forward to the enhancing phase, we start by splitting the initial reconstruction of  $x$ , i.e.  $\hat{x}$ , into non-overlapping blocks. A small block size (e.g.  $4 \times 4$  pixel blocks) is desirable for generation of an accurate prediction. By using a small size block, we increase the chances of having correlated blocks.

For each  $K \times K$ -pixels  $b$ -block of the initial reconstructed image  $\hat{x}$ , we consider its 8 surrounding blocks  $b_i \{i \in \{1, 2, \dots, 8\}\}$  as shown in Figure 2. The intensity of samples of block  $b$  and its surroundings will be used for the prediction estimation. We use the Sum of Absolute Difference (SAD) as a criterion in order to measure the similarity between block  $b$  and its neighbors,

$$\text{SAD}_{i \in \{1, \dots, 8\}} = \sum |b_i - b|. \quad (5)$$

Using this criterion and a prescribed threshold  $T$ , the neighboring blocks which have the most similarity to the block  $b$  are identified for the contribution in generating a prediction for  $b$ ,

$$\text{SAD}_{i \in (1, \dots, 8)} < T. \quad (6)$$

The threshold  $T$  is correlated to the block size and the initial image representation domain (maximal intensity value within the image). The weighting is used to control the influence each sample has on the prediction process depending on its position in the surrounding area. The weighting function allows us to emphasize the pixels which are closer to current block and thus more important for the prediction. A good choice for the weighting function is Hamming function [13] which is depicted in Figure 3. The size of window is considered as  $3K \times 3K$ . By splitting this window into  $K \times K$  blocks, the weights for the surrounding blocks of  $b$  are obtained. These weights regulate the pixels influence in the prediction process.  $\square$

The correlation among adjacent blocks is exploited to provide an accurate prediction for current block  $b$  using following equation:

$$\tilde{b} = \frac{b + \sum_{k \in L} b_k \cdot w_k}{w + \sum_{k \in L} w_k}, \quad (7)$$

TABLE 1. IMAGE RECONSTRUCTION QUALITY IN PSNR(DB)

B	Algorithm	Subrate				
		0.1	0.2	0.3	0.4	0.5
Peppers						
16	BCS-SPL	28.73	31.67	33.51	34.94	36.26
	BRCS	<b>28.83</b>	<b>31.80</b>	<b>33.64</b>	<b>35.06</b>	<b>36.37</b>
32	BCS-SPL	28.99	32.01	33.73	35.12	36.37
	BRCS	<b>29.16</b>	<b>32.24</b>	<b>33.98</b>	<b>35.36</b>	<b>36.62</b>
64	BCS-SPL	29.38	32.19	33.88	35.22	36.48
	BRCS	<b>29.64</b>	<b>32.52</b>	<b>34.25</b>	<b>35.60</b>	<b>36.86</b>
Lena						
16	BCS-SPL	27.61	30.89	33.08	34.83	36.48
	BRCS	<b>27.66</b>	<b>30.95</b>	<b>33.15</b>	<b>34.90</b>	<b>36.54</b>
32	BCS-SPL	28.08	31.35	33.46	35.19	36.75
	BRCS	<b>28.16</b>	<b>31.45</b>	<b>33.59</b>	<b>35.32</b>	<b>36.89</b>
64	BCS-SPL	28.51	31.60	33.64	35.32	36.87
	BRCS	28.62	31.76	33.84	35.53	37.10
Barbara						
16	BCS-SPL	22.63	23.92	25.43	26.95	28.65
	BRCS	<b>22.65</b>	<b>23.96</b>	<b>25.48</b>	<b>27.01</b>	<b>28.73</b>
32	BCS-SPL	22.62	24.13	25.67	27.21	28.82
	BRCS	<b>22.65</b>	<b>24.19</b>	<b>25.75</b>	<b>27.32</b>	<b>28.96</b>
64	BCS-SPL	22.79	24.39	25.77	27.22	28.78
	BRCS	<b>22.83</b>	<b>24.48</b>	<b>25.90</b>	<b>27.38</b>	<b>28.98</b>
Mandrill						
16	BCS-SPL	20.68	21.84	22.89	23.94	25.08
	BRCS	<b>20.70</b>	<b>21.86</b>	<b>22.90</b>	<b>23.95</b>	<b>25.08</b>
32	BCS-SPL	20.68	21.86	22.89	23.95	25.08
	BRCS	<b>20.70</b>	<b>21.89</b>	<b>22.91</b>	<b>23.97</b>	<b>25.10</b>
64	BCS-SPL	26.98	28.91	30.38	31.74	33.08
	BRCS	<b>27.05</b>	<b>29.07</b>	<b>30.59</b>	<b>31.98</b>	<b>33.37</b>

TABLE 2. RECONSTRUCTION TIME AND QUALITY FOR LENA

Subrate	Algorithm	Time(s)	PSNR(dB)

<b>0.1</b>	<b>BCS-SPL</b>	72.86	28.08
	<b>BRCS</b>	99.29	28.16
<b>0.2</b>	<b>BCS-SPL</b>	30.61	31.35
	<b>BRCS</b>	45.50	31.45
<b>0.3</b>	<b>BCS-SPL</b>	21.63	33.46
	<b>BRCS</b>	35.33	33.59
<b>0.4</b>	<b>BCS-SPL</b>	21.41	35.19
	<b>BRCS</b>	30.66	35.32
<b>0.5</b>	<b>BCS-SPL</b>	12.01	36.75
	<b>BRCS</b>	27.57	36.89

where  $L$  is the set of the neighboring blocks which hold (6) and  $w_k$  are the weights for the blocks belonging to  $L$ ;  $w$  is the central window in the weighting function. This prediction process is done for all blocks of the image in order to obtain the prediction  $\tilde{x}$ . It should be noted that for the border-positioned blocks the missing surrounding blocks are obtained by mirroring of the existing ones. Once the prediction image  $\tilde{x}$  is obtained, it is further sampled by the same procedure in (1), using the initial measurement matrix  $\Phi$ , to produce the predicted measurements  $\tilde{y}$ . At the next step, the difference between  $y$  and  $\tilde{y}$  is determined and known as the measurement-domain residual. The residual signal produced by such method is much more compressible, when compared to the original measurements  $y$  [12].

Finally, this residual drives the CS reconstruction to recover the image-domain residual coefficients  $x_r$ ,

$$x_r = \text{CS-Reconstruction}(y - \tilde{y}, \Phi). \quad (8)$$

The final reconstructed image is produced by adding the prediction and the reconstructed residual together,

$$\hat{x} = x_r + \tilde{x}. \quad (9)$$

### III. EXPERIMENTAL RESULTS

The performance of the proposed RCS algorithm is evaluated on 5 popular 8 bits per pixel, grayscale test images (*Lena*, *Peppers*, *Barbara*, *Mandrill* and *Goldhill*) of  $512 \times 512$  pixels resolution. All results are averaged over 5 independent trials because of the random nature of the measurement matrix  $\Phi$ . We make the assessment in terms of the quality of the reconstructed image, i.e. PSNR (Peak Signal-to-Noise Ratio) and computational burden, i.e. reconstruction time. The block size used for splitting the initial image prior to the prediction generation is  $4 \times 4$ . The value 128 was finally considered for  $T$  in equation (5). The improvement from the initial reconstruction is depicted in Table 1 where the BCS-SPL algorithm is coupled with the Double Discrete Wavelet Transform (DDWT) as sparsity basis ( $\Psi$ ). As mentioned before, the sampling in the BCS-SPL is achieved by splitting the image into the  $B \times B$  distinct blocks. Considering the CS

TABLE 3. RECONSTRUCTION QUALITY USING DIFFERENT TRANSFORMATIONS FOR LENA

Algorithm	Subrate				
	0.1	0.2	0.3	0.4	0.5

<b>DDWT</b>	28.16	31.45	33.59	35.32	36.89
<b>DWT</b>	27.78	30.92	33.05	34.77	36.34
<b>DCT</b>	26.23	30.26	32.72	34.47	36.08
<b>CT</b>	28.44	31.25	33.21	34.89	36.43

TABLE 4. RECONSTRUCTION TIME  
FOR AT SUBRATE 0.3

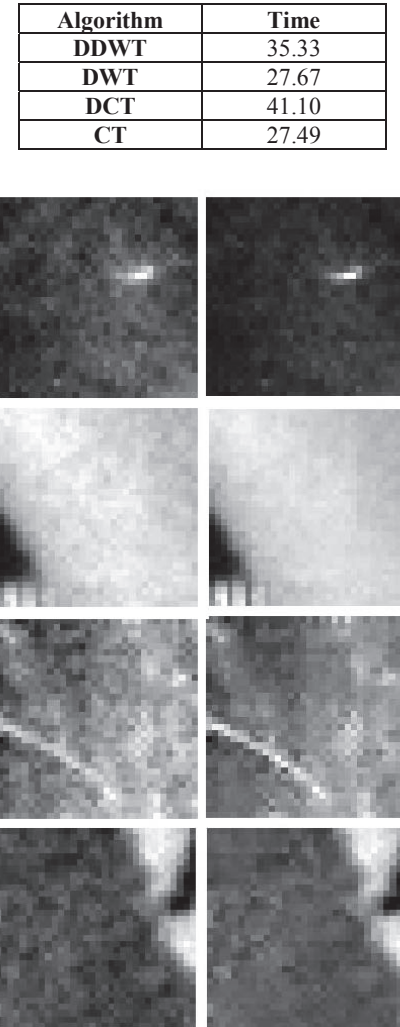


Fig. 4. 32×32 Blocks of the reconstructed images:  
left: initial, right: enhanced

acquisition of the image with the block sizes of 16×16, 32×32 and 64×64 pixels at any substrate (0.1 to 0.5), our algorithm is proven to bring an enhancement to the reconstructed image.

In Table 2, we present the trade-off between the reconstruction time and PSNR for "Lena" at various substrates ( $B = 32$ ). As expected, our algorithm cannot be faster than the BCS-SPL that it adds to, mostly due to prediction time.

In Table 3 and 4, we consider different sparsity basis transforms ( $\Psi$ ), i.e. DDWT, DWT, Discrete Cosine

Transform (DCT) and Contourlet Transform (CT) for the image "Lena". As can be seen, the DDWT is the most efficient one in terms of image quality and the CT transformation is the fastest one.

Visually, our algorithm smoothens the low-frequency areas and sharpens the edges, as seen in Fig. 4.□

#### IV. CONCLUSION

In this paper, we exploited and combined the fundamental principle of CS reconstruction and the high degree of spatial correlation of images; the former through residual reconstruction and the latter through block prediction. The core of the proposed algorithm is creating a prediction comparable to the original signal using the neighboring blocks of a block in an intra-prediction scheme. This prediction is used to produce a measurement-domain residual which is more compressible, thus enhancing the quality of the image.

#### REFERENCES

- [1] E. J. Candes and M. B. Wakin, "An introduction to compressive sampling," *IEEE Signal Processing Mag.*, vol. 25, pp. 21-30, March 2008.
- [2] D. L. Donoho, "Compressed Sensing," *IEEE Trans. Information Theory*, vol.52, no.4, pp.1289-1306, 2006.
- [3] S. S. Chen, D. L. Donoho, and M. A. Saunders, "Atomic decomposition by basis pursuit," *SIAM J. Scientific Computing*, vol. 20, no.1, pp. 33-61, Aug. 1998.
- [4] S. Mun and J. E. Fowler, "Block compressed sensing of images using directional transforms," in *Proc. Int. Conf. Image Processing (ICIP)*, Cairo, Egypt, Nov. 2009, pp. 3021-3024.
- [5] L. Gan, "Block compressed sensing of natural images," in *Proc. Int. Conf. Digital Signal Processing*, Cardi\_, UK, pp. 403- 406, July 2007.
- [6] C. Chen, E. W. Tramel, and J. E. Fowler, "Compressed sensing recovery of images and video using multi-hypothesis predictions," in *Proc. 45th Asilomar Conf. on Signals, Systems, and Computers, Pacific Grove, CA*, Nov. 2011, pp. 1193-1198.
- [7] J. Zhang, D. Zhao, F. Jiang and W. Gao, "Structural group sparse representation for image compressive sensing recovery," in *Proc. IEEE Data Compression Conf.*, Snowbird, Utah, USA, Mar. 2013, pp. 331-340.
- [8] J. Zhang, D. Zhao, and F. Jiang, "Spatially Directional Predictive Coding For Block-Based Compressive Sensing Of Natural Images," *20th IEEE Int. Conf. Image Processing (ICIP)*, Melbourne, VIC, 2013, pp. 1021-1025,
- [9] J. Mota, N. Deligiannis, and M. Rodrigues, "Compressed sensing with side information: Geometrical interpretation and performance bounds," *IEEE Global Conf. Signal and Information Processing (GlobalSIP)*, Atlanta, GA, Dec. 2014, pp. 512-516.
- [10] M. Trocan, T. Maugey, J.E. Fowler, and B. Pesquet-Popescu, "Disparity-Compensated Compressed-Sensing Reconstruction for Multiview Images," *IEEE Int. Conf. Multimedia and Expo (ICME)*, Suntec City, July 2010, pp. 1225-1229.
- [11] M. Trocan, T. Maugey, E.W. Tramel, J.E. Fowler, and B. Pesquet-Popescu, "Compressed Sensing Of Multiview Images Using Disparity Compensation," in *Proc. of 17th IEEE Int. Conf. Image Processing*, Hong Kong, Sep. 2010., pp. 3345-3348.
- [12] M. Trocan, E. Tramel, J. Fowler, and B. Pesquet-Popescu, "Compressed-sensing recovery of multiview image and video sequences using signal prediction," *Multimedia Tools and Applications*, vol. 72, no. 1, 2013, pp. 95-121.
- [13] Shaunak Ganguly, Shaumik Ganguly and M. Trocan, "An Overlapped Motion Compensated Approach for Video Deinterlacing," *6<sup>th</sup> Int. Conf. Computational Collective Intelligence (ICCI)*, Seoul, Korea, Sep. 2014, pp. 644-652.